EUSAR 2021; 13th European Conference on Synthetic Aperture Radar, 29 March-1 April 2021, Online
https://ieeexplore.ieee.org/abstract/document/9472656

Multistatic Dual-Polarimetric Through-Wall 3D-SAR

Daniel Andre[a], Francis Watson[b], Mark Finnis[c]
[a] Centre for Electronic Warfare Information and Cyber, Cranfield University, Defence Academy of the United Kingdom, Shrivenham, UK
[b] Dstl, Porton Down, UK
[c] Centre for Defence Engineering, Cranfield University, Defence Academy of the United Kingdom, Shrivenham, UK

Abstract

Through-wall (TW) imaging is of great interest for both military and civilian applications. At sufficiently low radar frequencies, Synthetic Aperture Radar (SAR) provides a TW sensing solution, however making sense of cluttered and overlaid signatures can prove difficult. This work investigates the suitability of three-dimensional dual-polarimetric multistatic TW-SAR, for the determination of building architectures and the detection of targets within buildings. These results are relevant to radar sensing Unmanned Air Systems under current development.

1 Introduction

Through-wall (TW) imaging is of great interest for both military and civilian applications [1]. At sufficiently low radar frequencies, Synthetic Aperture Radar (SAR) provides a TW sensing solution, however making sense of cluttered and overlaid signatures can prove difficult, especially when the target building comprises several floor levels.

Using Cranfield University's Ground-Based SAR (GBSAR) facility [2,3], the suitability of three-dimensional dual-polarimetric multistatic TW-SAR, for the determination of building architectures and the detection of targets within buildings is investigated. These results are relevant to radar sensing Unmanned Air Systems (UAS) under current development [4], amongst others.

The measurement setup is described in section 2. Two-dimensional (2D) image TW results are presented in section 3.1 and three-dimensional (3D) image results are presented in section 3.2, followed by the conclusion.

2 Measurement

Measurements were conducted at the Cranfield University GBSAR laboratory [2,3]. A concrete walled structure was erected comprising of three partitioned areas, as shown in **Figure 1**. Measurements were conducted in the 1-6 GHz range, these providing sufficient, but varying levels of Radio Frequency (RF) penetration through the concrete.

The 2D SAR imagery consisted of five collections: one monostatic and four bistatic. The monostatic scan consisted of a 3.5 m horizontal scan; the four bistatic geometries were achieved by placing the receiver at four fixed locations about the scene. The scanner and an example fixed receiver location are pictured in **Figure 2** top. Whilst in a real radar sensing Unmanned Air System (UAS), various receivers would be functioning simultaneously, in the Laboratory setup, the different geometries are scanned sequentially. As long as the scene is left undisturbed, the combined collections are equivalent to a single multistatic collection.

For the 3D SAR imagery, the geometry was the same as for the 2D, except that the scanner also scanned in the vertical dimension with an aperture of 60 cm.

A schematic of the target and multistatic geometry can be seen in Fig.2 bottom. The transmitter 2D aperture can be seen in red, whereas the four fixed receiver locations are indicated by the star symbols. The midpoint locations between the transmitter and receiver are marked in green, and these are referred to here as the *equivalent monostatic* apertures (EqM). It can be seen that by varying the position of the receiver, the EqM is also moved about the scene.

Two metal objects were placed in the structure: a barrel and a briefcase. Their locations can be seen in the **Figure 2** schematic.

Figure 1 Concrete building structure

3 Results

TW SAR results for both linear scans and 2D aperture scans are presented. Example results for individual bistatic geometries and for the combined multistatic scans are presented. Here, a simple SAR Backprojection image formation algorithm is implemented, without wall refractive index compensation.

3.1 2D SAR results

Two example 2D bistatic SAR HH polarisation results are presented in **Figure 3**. These figures have the scene schematic overlaid, as well as the radar geometry: the red line represents the scanned transmitter positions, the blue the fixed receiver position, and the green line represents the midpoint of these, referred to as the EqM aperture.

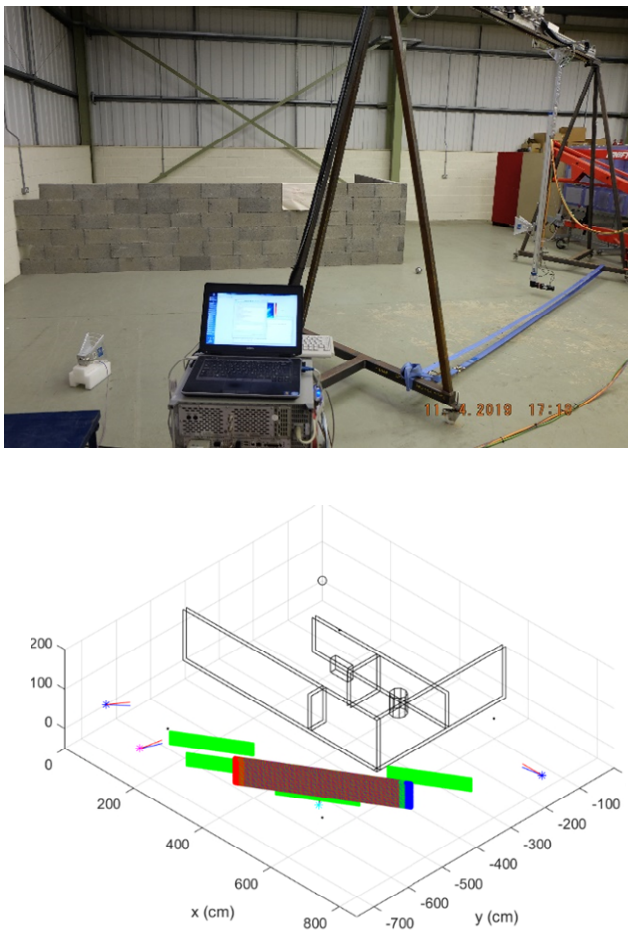

Figure 2 GBSAR scanning system and target, photograph (top) and schematic (bottom), the equivalent monostatic apertures can be seen in green.

The two bistatic geometries give significantly different results: different sides of the target structure are responding brightly. The brightest responses can be understood in terms of a specular flash response, these generally appearing bright in a SAR image, when the target surface normal intersects with the EqM.

In Figure 1 top for example, the internal wall next to the doorway is responding brightly as its surface normal intersects the EqM. In **Figure 2** bottom, the briefcase is responding brightly, again because the briefcase surface normal intersects the EqM.
In both geometries the barrel responds brightly, and there is an associated multipath signature seen in **Figure 1** top.
Both 2D SAR images are subject to overlay projection errors, as well as clutter overlay.

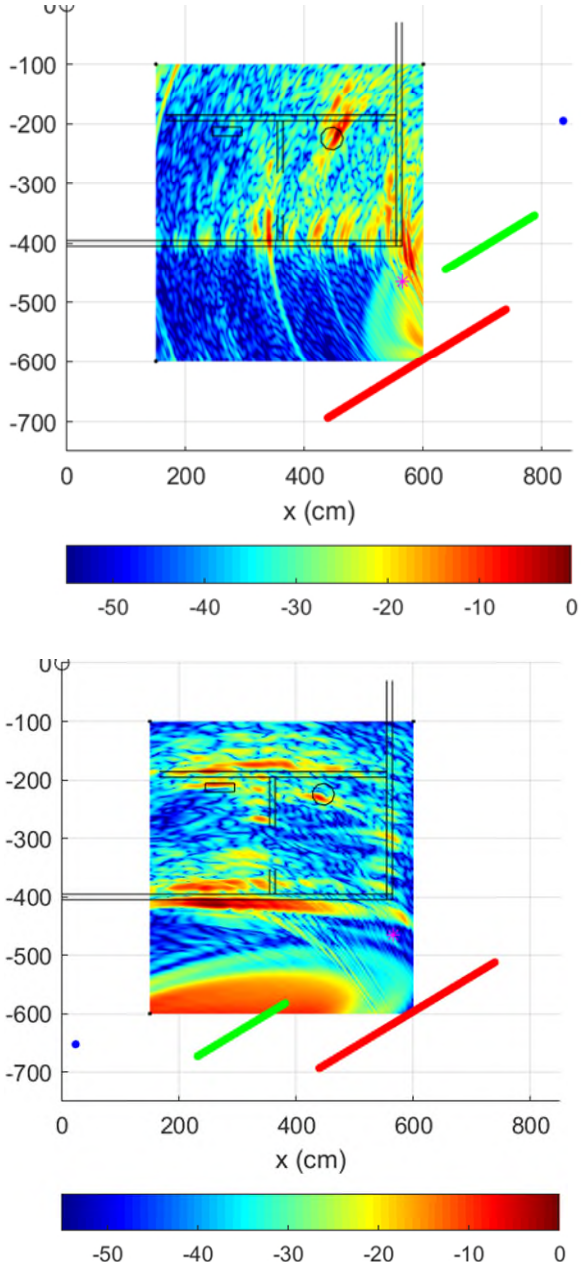

Figure 3 Example HH-polarisation 2D bistatic SAR intensity images (normalised dB) with scene schematic and radar geometry overlaid.

It is also noted that the TW signatures are subject to down-range shifts due to the reduced speed of the electromagnetic waves within the concrete walls, so that signature positions do not match precisely with the schematic.
The five multistatic geometries, as well as the two polarisations HH and VH, are combined into a single composite SAR image in **Figure 4**.
It can be seen that due to the spread of EqM apertures, that a large number of the target scene surfaces can be seen in the image. The exception to this is the wall to the top-right of the image, where no EqM aperture is available to intersect with the normal to that wall.

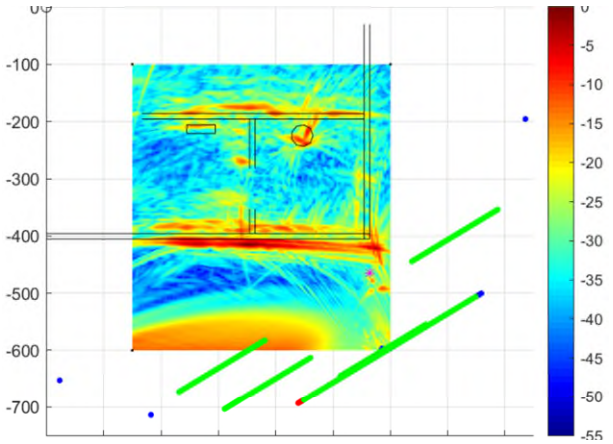

Figure 4 Multistatic dual-polarisation composite 2D SAR image (normalised dB) with target schematic and radar geometries overlaid.

3.2 3D SAR results

Two example HH polarisation 3D bistatic SAR results are presented in **Figure 5** for the receiver on right, and **Figure 6** for the receiver on far left. In **Figure 5** projections of the volumetric image can be compared with the iso-brightness contour rendering. The brightest features are similar to those present in the 2D SAR images of **Figure 3**, however these are now resolved in the vertical. The clutter which had originated from above the scene, for example from the laboratory ceiling, is now not present in these images.
The observation that scatterer surfaces respond brightly when their surface normal intersect the EqM applies here as well, also applying to the vertical dimension.
In the 3D SAR images, projection errors are no longer present, however in these results, the reduced electromagnetic wave propagation speed in the concrete walls has not been taken into account, so that TW scatterer signatures are shifted down-range in the imagery, from their true positions.
The five multistatic geometry HH polarisation images are combined into a single composite SAR image in **Figure 7**. All parts of the target structure are well represented in the image apart from those whose surface normals do not intersect with any EqM aperture.

In **Figure 8** the multistatic results have been combined for the HH and VH polarizations. The co and cross-polarizations have been given different colour maps. Some features are brightest in the cross-polarisation. The multipath between the barrel and the inner wall for example gives a large cross-polar response.

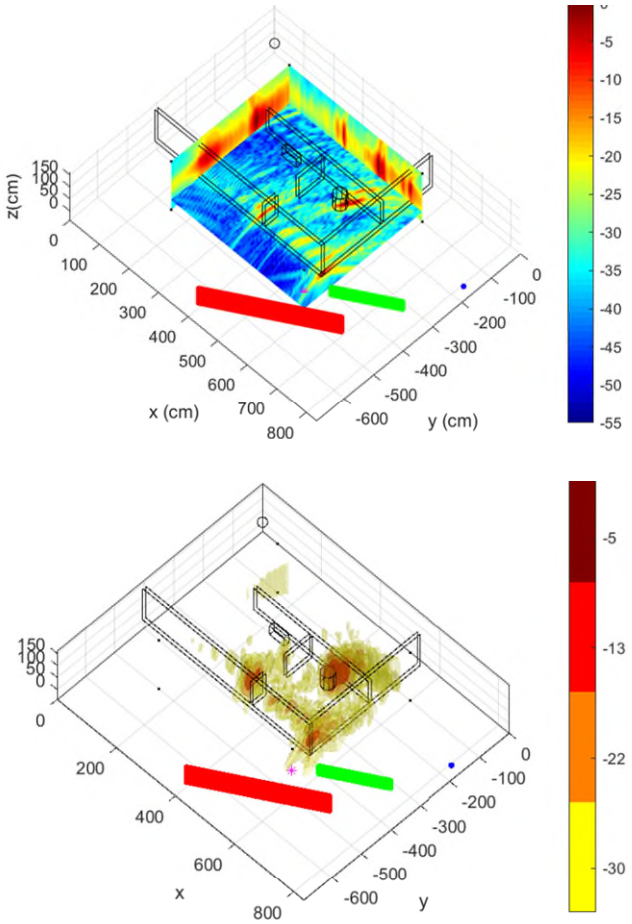

Figure 5 Example HH-polarisation renderings of a bistatic volumetric SAR image, receiver on right. Top image shows projections, bottom image shows iso-brightness contours. (normalised dB)

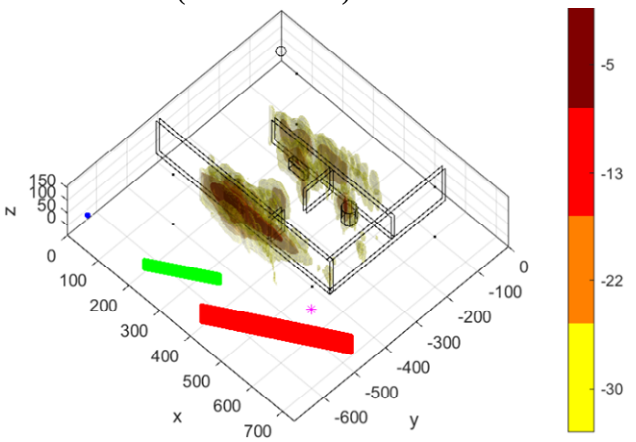

Figure 6 Example HH-polarisation renderings of bistatic volumetric SAR image, receiver on far left, with scene schematic and radar geometry overlaid. (normalised dB)

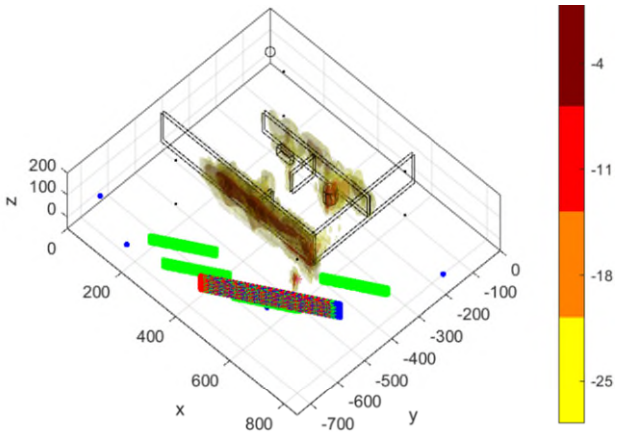

Figure 7 Multistatic HH-polarisation composite 3D SAR image (normalised dB) with target schematic and radar geometries overlaid.

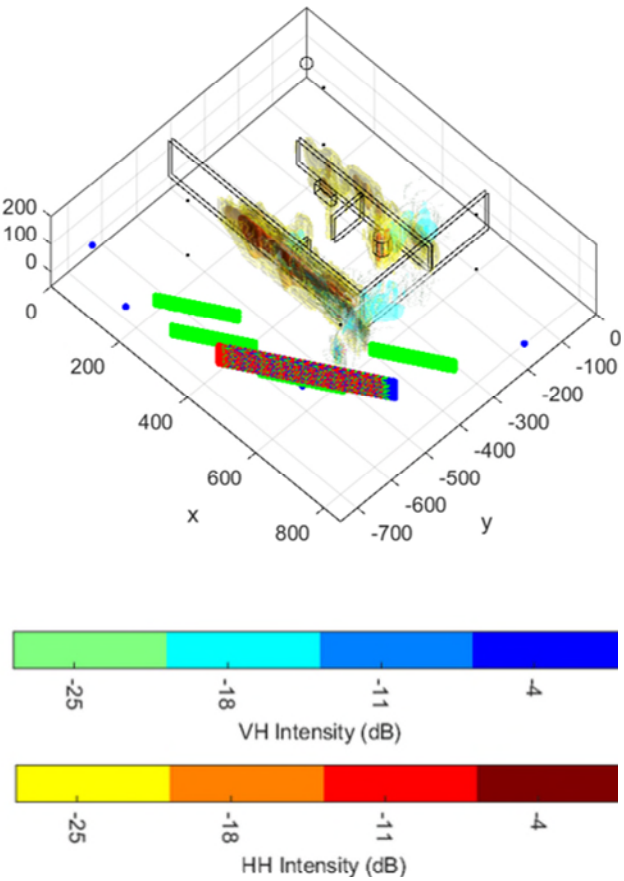

Figure 8 Multistatic dual-polarisation composite 3D SAR image with target schematic and radar geometries overlaid. (normalised dB)

4 Conclusion

Initial 2D and 3D TW multistatic and dual-polarimetric SAR measurements of a building-like target scene have been conducted at the Cranfield University GBSAR laboratory.

2D SAR images were subject to projection errors and clutter overlay from heights outside of the region of interest, a problem which would be exacerbated with multi-floor buildings.

3D SAR imagery did not suffer from projection errors, and the clutter from outside-scene heights is not present.

It has been found that scene structures respond most brightly in imagery when the target surface normal intersect EqM apertures, hence capturing the specular flash. Therefore with a sufficient dispersal of receivers about the scene, a substantial proportion of the scene could be made visible in combined multistatic data.

In this work, two polarisations were collected, however future work will involve full polarimetric collections allowing the investigation of multiple polarimetric decompositions and their combinations into useful multistatic composites.

This work helps to inform the development of radar sensing UAS platforms [4].

Acknowledgment

We thank David Blacknell, Darren Muff, Matt Nottingham, and Claire Morris for useful technical discussions, and Cemex UK for donating the concrete blocks for the research. This work was funded by Dstl.

5 Literature

[1] Haas A., Aerospace G. Characterization of building structures with SAR. EUSAR 2018: 12th European Conference on Synthetic Aperture Radar, Proceedings of. Aachen, Germany: VDE; 2018.

[2] Andre, D: Faulkner, B: Finnis, M: Low-frequency 3D synthetic aperture radar for the remote intelligence of building interiors, Electronic Letters, 53 (15) 984-987, 2017.

[3] Corbett, B: Andre, D: Finnis, M: Through-wall detection and imaging of a vibrating target using synthetic aperture radar, Electronic Letters, 53 (15) 991-995, 2017.

[4] Price, G.: Moate, C.: Andre, D.: Finnis, M: Comparison of Compressive Sensing Techniques for Multistatic SAR Image Formation and Exploitation, NATO SET-265, Salamanca, May 2019.